FREEFORM FABRICATION OF ZINC-AIR BATTERIES AND ELECTROMECHANICAL ASSEMBLIES

Evan Malone, Kian Rasa, Daniel Cohen, Todd Isaacson, Hilary Lashley, Hod Lipson

Computational Synthesis Laboratory, Department of Mechanical and Aerospace Engineering, Cornell University, Ithaca NY 14853 USA
em224@cornell.edu

Keywords

battery, zinc, electromechanical, assembly, freeform, functional

Abstract

This paper reports on a fabrication platform and extensions to deposition-based processes that permit freeform fabrication of three-dimensional functional assemblies with embedded conductive wiring and power sources. Structure and joints are produced by fused deposition of thermoplastics and deposition of elastomers. Conductive wiring is achieved by deposition of various low-melting-point alloys and conductive pastes. Batteries based on zinc-air chemistry are produced by deposition of zinc, electrolyte, and catalysts, with separator media and electrodes. Details of the deposition processes are provided and several printed assemblies are demonstrated.

Introduction

In the last several years, there have been an increasing number of solid-freeform fabrication processes and materials being researched. It has not escaped the notice of some that this diversity is nearing the point at which almost any conventionally manufactured part could be made entirely via SFF processes, and that a synthesis of compatible processes may permit the fabrication of entire functional assemblies [Weiss and Prinz, 1998; Safari *et. al.,* 2000] and even complete functional systems [Lipson *et. al.*, 2000]. The Cornell Computational Synthesis Laboratory (CCSL) is investigating the freeform fabrication of functional, integrated, electromechanical systems, and an understanding of the interface between the design process and this new fabrication domain. A high-performance motion control platform and an initial set of tools have been designed and constructed that have enabled the exploration of layered fabrication processes in a wide variety of materials and material combinations. The materials experimented with thus far include thermoplastics, low-melting-point alloys, and a variety of gels and slurries. Here we report on freeform fabrication of a zinc-air battery which is capable of powering a small DC brush motor, thermoplastic and elastomer flexure joints, two approaches to embedded wiring, and structures with embedded wiring. These components are some of the basic building blocks necessary for freeform fabrication of three-dimensional, functional, electromechanical systems.

Fabrication Platform

In order to provide maximum freedom for experimentation with a wide variety of materials and processes, a custom robotic platform and two material deposition tools have been designed and constructed. The initial requirement employed in the design of these tools can be stated briefly as follows: the motion control platform should provide maximal parametric freedom to the deposition processes, and permit the sequential use of many deposition processes

in the course of fabricating a given object. The most significant assumption informing the design is that materials will be deposited as streams or droplets in a layered manufacturing process. Positioning is therefore limited to three Cartesian axes, and an emphasis was placed on velocity regulation, path-following and positioning accuracy, resolution, repeatability, and high acceleration to achieve fine features while printing at a constant material feed rate. Lower acceleration performance would require more complex deposition feedrate control. Table I describes the performance requirements employed in the design of the positioning system.

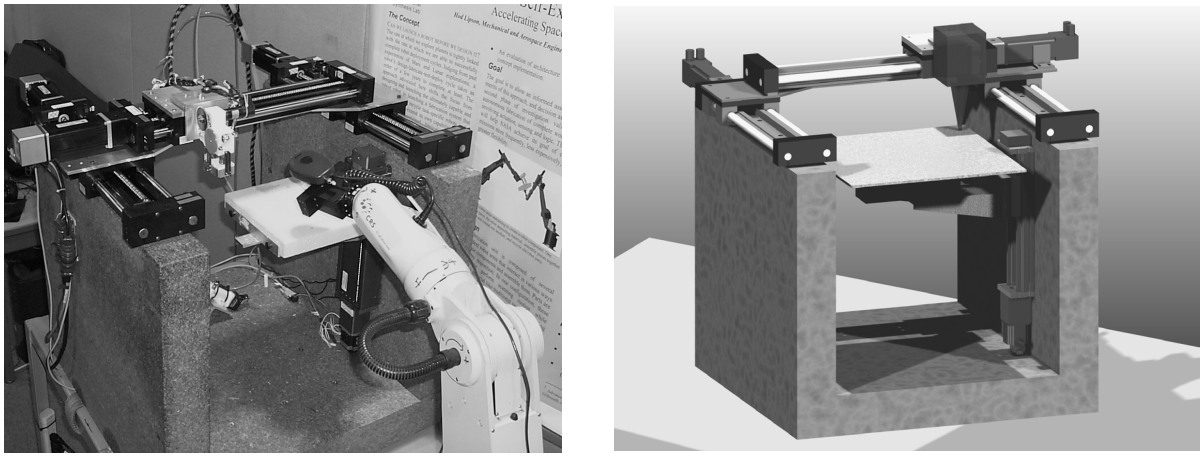


Figure 1: Gantry robot fabrication platform

A Cartesian gantry-configuration robot (Figure 1) has been selected for this application for its relatively simple control, large payload capacity relative to rigidity, and positioning/path-following performance. Linear motors, ballscrews, and cable-pulley systems were all considered for the drivetrain, and ballscrews were selected for simplicity. A cable-pulley system is an attractive alternative because the drive motors themselves do not need to be located on the moving components of the system.

Table I: Fabrication System Performance Specifications

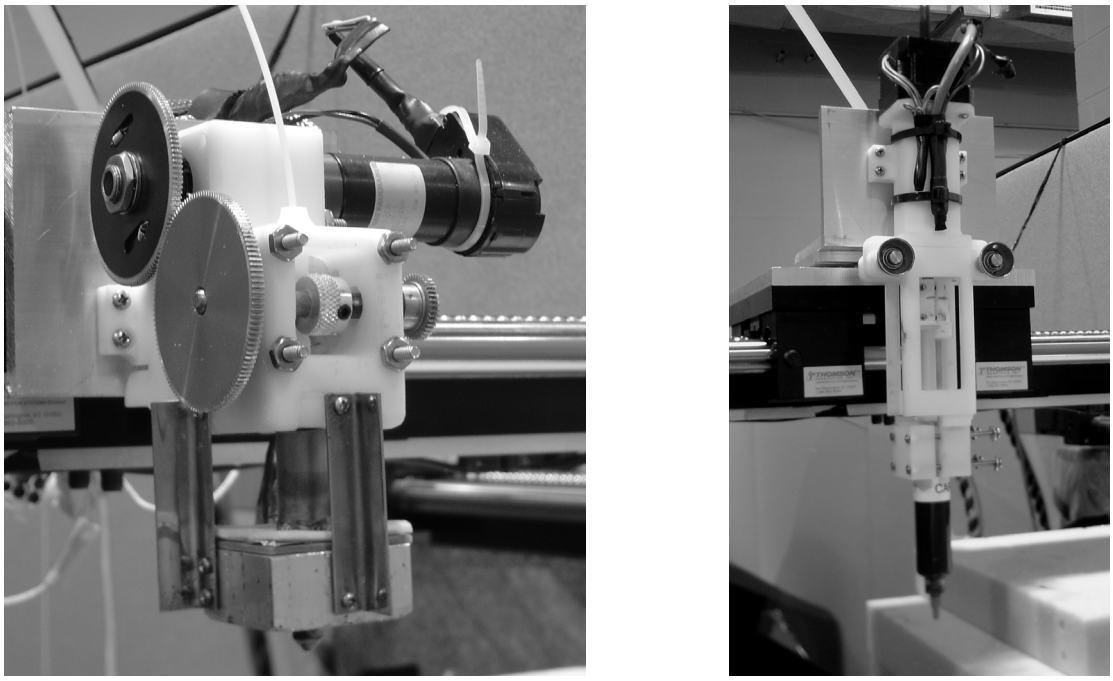
Minimum material stream/drop diameter	250	µm	0.010	in
Materials cross-section area	4.9×10^{-8}	m^2		
Build rate	2.5×10^{-9}	m^3/s	0.55	in^3/h
Nominal speed along path	0.05	m/s		
Min turn radius at nominal speed	125	µm	4.92×10^{-3}	in
Tool Position Accuracy (+/-)	25	µm	9.84×10^{-4}	in
Tool Position Repeatability (+/-)	25	µm	9.84×10^{-4}	in
Positioning Resolution	5	µm	1.97×10^{-4}	in
Build envelope x	0.3	m	11.8	in
Build envelope y	0.3	m	11.8	in
Build envelope z	0.3	m	11.8	in
Max XY acceleration	20.75	m/s^2	2.12	g

A software application has been created to manage path planning and control. Multi-material objects are defined using multiple STL (stereolithography) files, each describing a single material. Each material is associated with a deposition tool and material properties governing layer thickness, deposition width and deposition rates. Geometry slicing and path generation algorithms construct unique perimeter contour- and fill raster-paths based on the

tools' and materials' parameters, and combine the layers into a fabrication sequence with increasing height. Special care is needed to prioritize layers of similar heights according to interaction among materials.

Deposition Tools

A freeform fabrication system capable of producing complex, functional products requires a highly versatile deposition tool or set of deposition tools to address the need to deposit a broad range of materials with vastly different physical properties. The set of materials explored in the freeform fabrication of batteries can be organized into four basic categories: plastics, metals, liquid chemicals, and chemical pastes. For the initial experiments, two separate deposition tools were designed – one for plastics and metals, and another for liquid chemicals and pastes. The tools were designed to be compatible with both a Cartesian robot and a six-axis robotic arm in order to allow for experimentation with both types of positioning systems. Load restrictions and dimensional limitations of robotic arms require that tools be small and lightweight, a feature that also leads to lower systemic inertia and enhanced robotic performance.



(a) (b)

Figure 2: Extrusion tools constructed: (a) wire-fed extruder, and (b) syringe tool

The deposition tool for metals and plastics (Figure 2a) is an extruder that feeds material in wire-form (0.050" – 0.070" diameter) through an actively air-cooled metal guide-tube and into a heated liquefier block containing a nozzle [Swanson *et. al.* 1999]. The tool has been successfully tested with solid core Pb-Sn solder wire, as well as ABS (acrylonitrile-butadiene-styrene) thermoplastic wire.

A separate tool was designed to deposit liquids and chemical pastes (Figure 2b). This tool accepts standard commercial 10cc Luer-lock syringe barrels and plungers. The plunger position is actuated by a linear stepper-motor capable of exerting 50 lbf. Prior experiments with a pneumatic dispensing system proved open-loop pressure control to be unsuitable for freeform

deposition of slurries; instead, volumetric control provided by the current approach is more broadly applicable, and also allows for more precise reverse-flow control. The design of the tool simplifies experimentation with a broad range of materials. Materials may be easily changed by substituting a different syringe barrel and plunger in the plunger-driver component of the tool.

Freeform Fabrication of a Zinc-Air Battery

The freeform fabrication of a functional battery was selected as a comprehensive test of the multiple material capabilities of the previously described platform. There is little literature on the production of freeform, three-dimensional energy storage devices, though a planar thin-film cell has recently been demonstrated by Power Paper Ltd. (2003) for low-power applications. Freeform fabricated batteries are a major step toward freeform fabricated, active, functional, electromechanical systems. The size, shape, and performance of a cell become free design parameters, and can be customized for the specific geometry and functional requirements of a product. A cell can be placed at arbitrary locations within the product, rather than forcing the design of a product to be limited by the characteristics of commercially available energy sources. With this in mind, research and experiments were conducted in an effort to produce a freeform cell. For the purpose of these experiments, a cell is defined as a device that converts the chemical potential energy between its anode and cathode materials into electrical energy by means of redox reactions: reduction (electron gain) at the cathode, oxidation (electron loss) at the anode. A battery is comprised of one or more connected cells. The essential components of a Zn-air cell are the negative terminal, anode, separator, cathode catalyst, cathode, positive terminal, and electrolyte (Table II, Figure 6).

Table II: Key Battery Components / Materials Tested*

Cell Component	Materials Tested
Electrolyte	0.25 Molar -> 8 Molar solution of potassium hydroxide (KOH) and distilled water
Negative terminal	Paste of methylcellulose (MC) with copper (Cu, 99% purity 2-5 μm), or with silver (Ag, 99% purity 1 μm)
Anode	Slurry of electrolyte with zinc (Zn, 97.1% purity, dust) and surfactant
Separator	Paper, or Rescor 740 insulating ceramic foam (Cotronics Inc.)
Cathode catalyst	Slurry of carbon black, manganese dioxide (MnO_2, 80-85% purity), and electrolyte
Cathode	Air
Positive terminal	Paste of methylcellulose with nickel (Ni, 99% purity -325 mesh), or copper, or silver

* Many of these materials are hazardous, and should only be handled with proper training and protective equipment

Zinc-air cell chemistry was the first considered because of its simplicity and high energy density. The basic chemical reactions are:

At Air Cathode: $\frac{1}{2} O_2 + H_2O + 2e \rightarrow 2OH^-$

At Zn Anode: $Zn \rightarrow Zn^{2+} + 2e$

$Zn^{2+} + 2OH^- \rightarrow Zn(OH)_2$

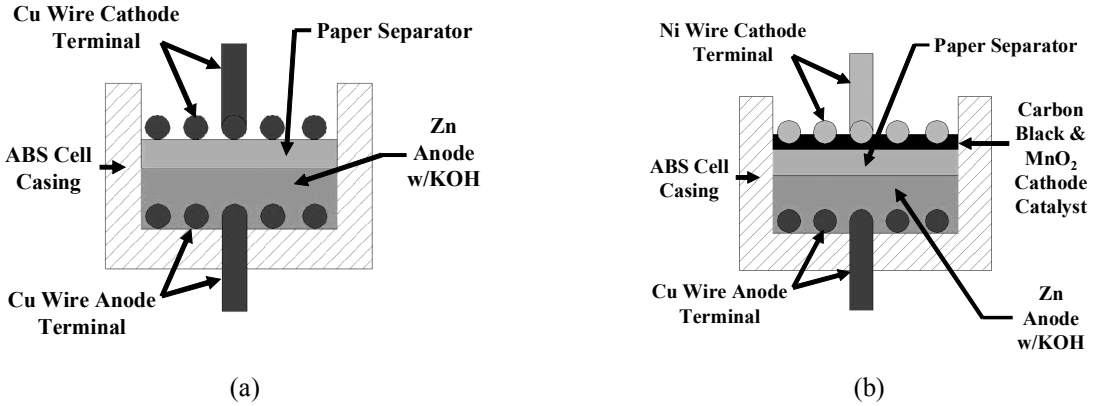
$Zn(OH)_2 \rightarrow ZnO + H_2O$

Overall: $\mathbf{Zn + \frac{1}{2}O_2 \rightarrow ZnO : E_0 = 1.65\ V}$

The experiments outlined below investigate the effects on cell performance of electrolyte concentration, current collector composition and geometry, cell structure and construction, and cathode catalyst composition. After the initial tests were conducted and the fundamental characteristics understood, the research shifted to adapting a battery design to solid-freeform fabrication processes.

Zn-Air Electrolyte Experiments

Tests were conducted with the aim of understanding the basic anode and electrolyte chemical ratios and concentrations, and all other variables were held constant. The test procedure [Isaacson, 2003] included mixing the Zn with various concentrations of KOH (0.25M to 8M) and placing the mixtures in an ABS cell casing, using copper wire as both the negative and positive terminals (Figure 3a).



(a) (b)

Figure 3: Experimental cells, in cross-section: (a) basic Zn-air cell and (b) Zn-air cell with MnO_2-carbon black catalyst

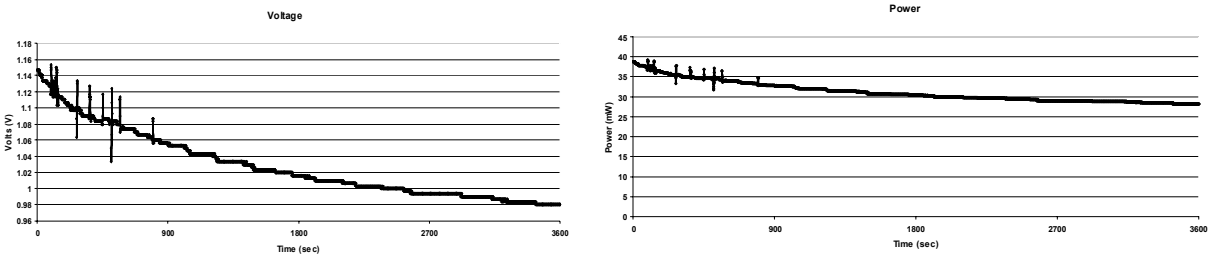
Paper was initially used as a separator for simplicity and consistency. The cells were loaded with a 102 Ohm resistor and the voltage recorded. It was found that an electrolyte concentration of 7M to 8M gave the cell a more consistent voltage over its lifetime.

Catalyst Experiments

Manganese dioxide and carbon black were then added to the cell to improve cell performance [Tinker, 2002]. The ratio of MnO_2 to carbon was derived from manganese dioxide alkaline cells. These materials are also used as a catalyst in commercial Zn-air batteries [Linden *et. al*. 2002; Duracell, 2001]. By weight, the anode was comprised of 65% Zn and 35% 8M KOH, the catalyst was comprised of 50% MnO_2, 44% 8M KOH, and 6% carbon black, and the separator layer consisted of 8M KOH saturated paper. The cell was constructed in a similar way to the previous cell design with the addition of a catalyst layer (Figure 3b), and tested in the same manner. Important observations made from these tests were that the consistency of cell performance improved and the voltage doubled compared to previous tests. The most significant observation was that the power output increased by 500%. To reduce the potential energy barrier at the terminal junctions, nickel and copper wire were used for the cathode and anode current collectors respectively.

Surface Area and Current Collector Experiments

Tests were conducted to understand the effects of surface area and increase overall performance. Using the same cell chemistry and mass of material as in previous tests, the cell surface area was increased from a 1" diameter to a 3" diameter, and the current collectors/terminals were doubled in length (6" coiled wire to a 12" coiled wire). The cells were loaded with a 33 Ohm resistor to acquire data relevant to the goal of running a 30mW electric DC brush motor. The graphs (Figure 4) below demonstrate that cells of this simple design are able to supply more than 30mW at 1V for more than ½ hour. The cells were able to turn the motor, and in doing so, validated the tested cell chemistry and structure.



(a) (b)

Figure 4: (a) Voltage vs. time of cell with increased surface area and current collector area and (b) power vs. time of cell with increased surface area and current collector area

Separator Experiments

Methylcellulose (MC) gel and Rescor 740 insulating ceramic foam were both tested for their efficacy as separator layers, to replace the only remaining unprintable component in the cells – paper. Methylcellulose (3 grams of MC to 100mL of 100°C distilled water) does not interact well with 8M KOH electrolyte [Danko, 1995] - the gel deteriorates and allows shorting between cathode and anode. Rescor 740 (100 parts base to 64 parts activator) is a permeable ceramic foam which absorbs the electrolyte and allows for the migration of ions across the layer, making it a viable choice as separator.

Extrusion Experiments

Conductive Pastes

Various metallic pastes and solder alloy were tested as materials for current collectors. Pb-Sn solder proved to be incompatible with the cell chemistry and was ruled out as a terminal material. MC was mixed in 1:1 ratios by mass with Cu, Ni, and Ag powders, and each was extruded through a syringe creating extrudable wires. Silver paste proved to be the best material for the cell terminals for two reasons; the silver terminals did not react with the cell chemistry and had lowest electrical resistivity of the pastes. This paste was thus used for both the anode and cathode current collectors/terminals. The nozzles used for testing were 14Ga stainless steel needles, which produced a stream approximately 1.4mm in diameter.

Separator

Surfactant was added to the Rescor 740 ceramic foam material to enable extrusion and to delay the curing of the material while in the syringe. The foam slurry is highly viscous and prone to phase separation, and requires a large diameter nozzle for successful extrusion. Initial

testing indicated that the addition of the surfactant in the separator material reduces power output slightly, and more testing is necessary to determine the optimum material and/or Rescor/surfactant ratio. The internal diameter of the nozzle used was 1.9mm, and the resulting stream of material was about 1.3mm in diameter.

Anode

The anode material (a slurry of Zn and KOH solution) was exceptionally difficult to extrude, as Zn settles out of the slurry and clogs the syringe. Surfactant was added to prevent clogging, but the resultant increase in ease of handling comes at the expense of some cell power output. Therefore, the slightest possible amount of surfactant was used. The anode consisted of 60% Zn, 30% KOH, and 10% surfactant by weight. The nozzle diameter was approximately 7mm, resulting in comparably-sized drops of deposited material.

Catalyst

The MnO_2 and carbon black powders are extrudable when pre-mixed with KOH solution. In order to achieve an homogeneous slurry, the catalyst material was forced through a syringe several times before use, using a pneumatic dispensing machine. 14Ga stainless steel syringe needles were used, and these produce a stream of about 1.4mm in diameter.

Freeform Fabricated Cell Design

The next round of experiments focused on the fabrication process. These tests were designed to demonstrate that 100% of the materials for a complete cell could be extruded, to

Table III: Process for Constructing a Manually Extruded Cell



Negative Terminal

The silver slurry was extruded into a container with a copper wire exposed to the silver for data collection purposes. It was then dried using a heat gun. The heat helps to evaporate the water from the MC solution and allows the material to be strong enough to receive the load of the next layer.



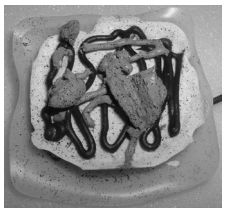
Anode

Here the Zn-KOH and surfactant slurry was added over the silver negative terminal.



Separator

For testing purposes, the Rescor separator layer was pre-cast. It was allowed to cure at room temperature for approximately five hours to ensure that the layer was solid and would not interfere with the other cell components and chemistry.



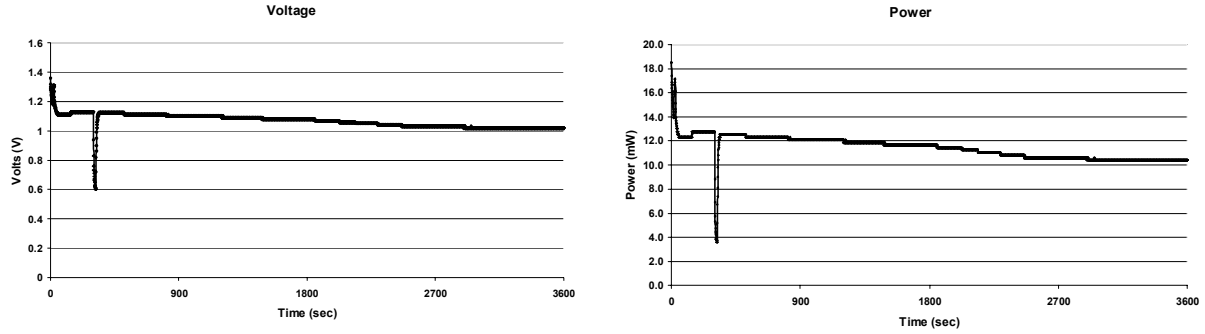
Catalyst and Cathode Terminal

Finally, after the separator was placed over the Zn, the catalyst was extruded freely over the separator. The silver slurry was then liberally extruded over the catalyst and separator. A copper wire (not shown) was placed over the silver cathode terminal for data collection purposes.

verify that freeform fabricated cell performance would be adequate (i.e. sufficiently powerful to turn the motor and have comparable voltage/power output to previously tested cells), and to identify problems that might occur during production with the fabrication platform.

Manually Extruded Cell and Results

Firstly, a cell was made by hand using only the extrudable materials and extrusion deposition. This process is detailed in Table III above. The graphs below (Figure 5) show the voltage and power output of the cell - loaded with a 100 Ohm resistor - over a one hour period.



(a) (b)

Figure 5: Performance of manually extruded cell; (a) voltage, and (b) power to 100 Ohm load.

The all-extruded cells have satisfactory performance, delivering more than 10mW at more than 1V for the entire hour of data collection. The downward spike in the graphs occurred when the cell was connected to the motor for demonstration testing. Multiple tests conducted with this cell design and manufacturing technique show repeatable results over a sample size of approximately six cells, suggesting the feasibility of producing a functional cell on the freeform fabrication platform.

Freeform Fabricated Cells

The first freeform fabricated cell design was essentially identical to that of the manually fabricated test cells. The zinc anode was surrounded by silver paste to enclose the zinc and prevent KOH evaporation, and to increase the reaction surface area of the negative terminal.

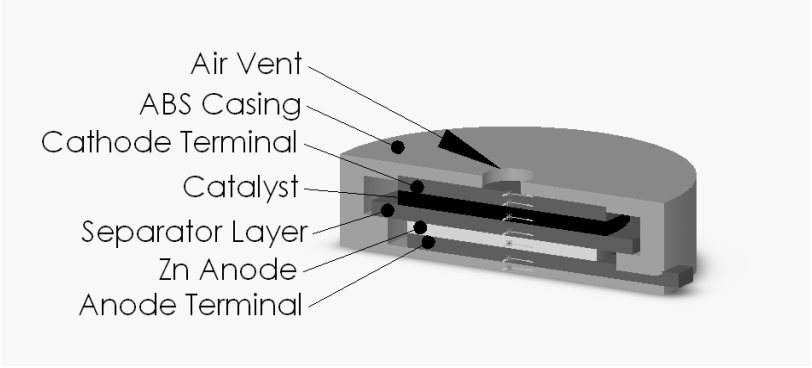


Figure 6: Cross-sectional view of freeform fabricated cell design

The separator layer was intentionally designed to be excessively large compared to the rest of the cell components to ensure that the cell did not short. The catalyst layer was extruded on top of

the separator layer, and the cathode terminal, constructed of MC/silver paste, was printed directly over the catalyst. Both the anode and the cathode terminals are connected to the motor or the data acquisition board via copper wires. The unenclosed cell was able to power the motor for about 2 seconds.

More recent experiments have focused on achieving encased cells. Figure 6 shows a cross-sectional view of a successfully fabricated, encased cell design. The internal structure is very similar to the unenclosed cells. The main functional difference in the designs is that the casing limits air diffusion into the cell, reducing the peak power output, but prolonging the life. Figure 7 highlights some key steps in the successful freeform fabrication of this encased cell design.

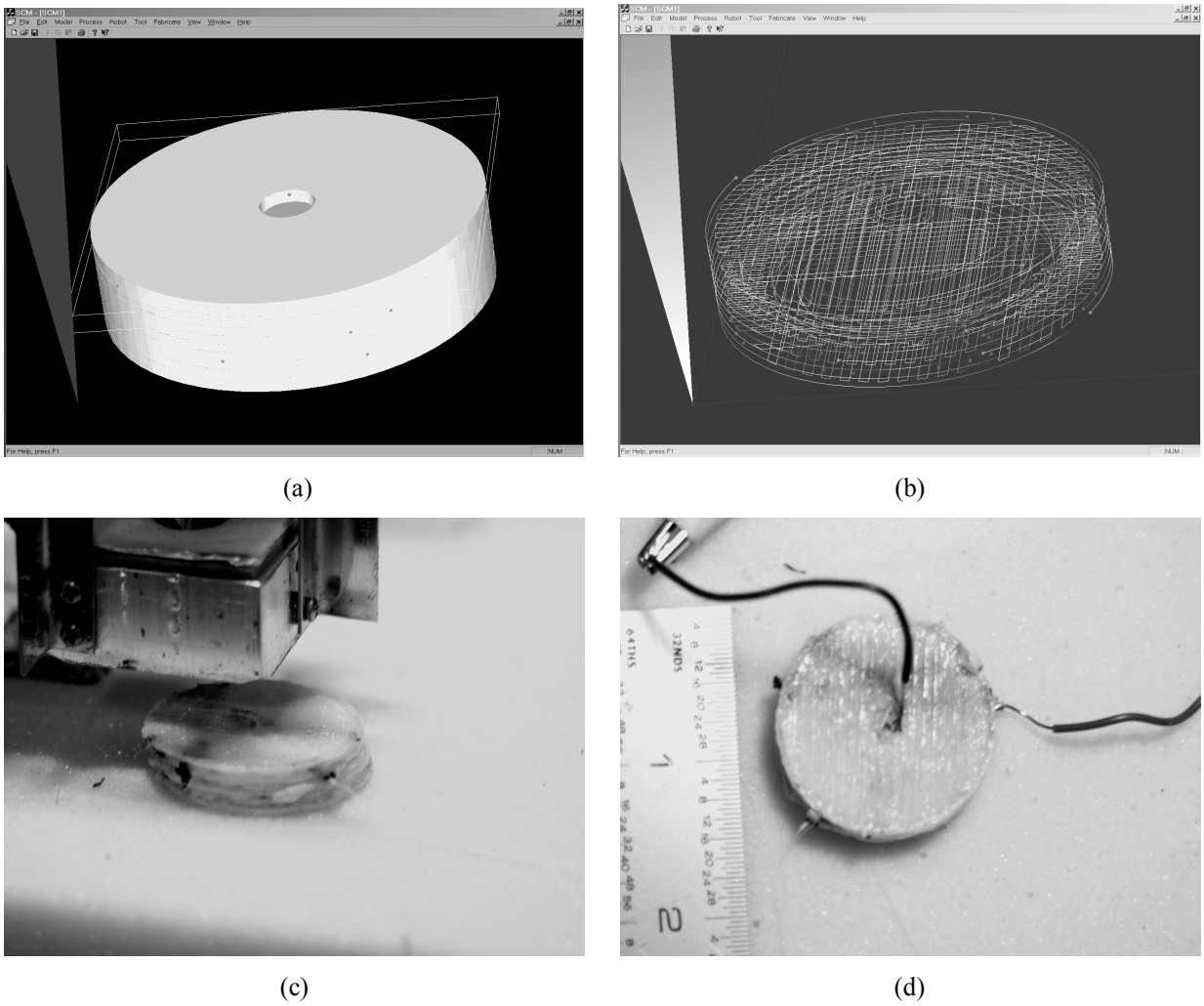


Figure 7: Sequence of operations in freeform fabrication of battery: (a) solid view of battery model in CCSL SCM software, (b) slicing of battery model in SCM application to generate tool paths, (c) final ABS layer printed, and (d) close-up photograph of completed battery.

Results and Discussion

The performance benchmark test for the freeform-fabricated cell was the ability to power a small DC brush motor, which consumes about 30mW, unloaded. An unenclosed cell has been produced which is able to provide the starting current for the motor, and to run the motor for

about 2 seconds. More recent experiments have focused on producing cells encased in thermoplastic, and a working cell encased in ABS has been produced (see Figure 7). Figure 8 depicts the power produced by this encased cell into a 100 Ohm load. Ongoing work will continue to optimize the active materials, material deposition tools, and cell geometric designs.

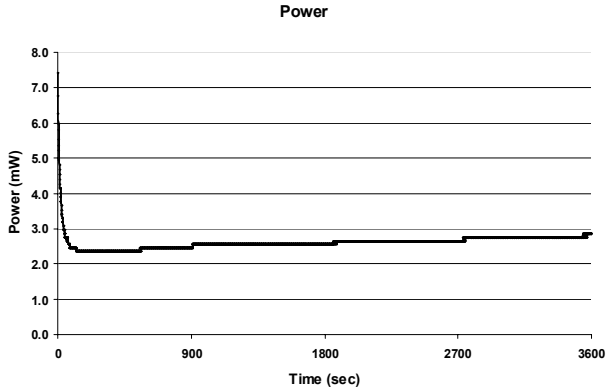


Figure 8: Power of ABS encased cell into 100Ω load

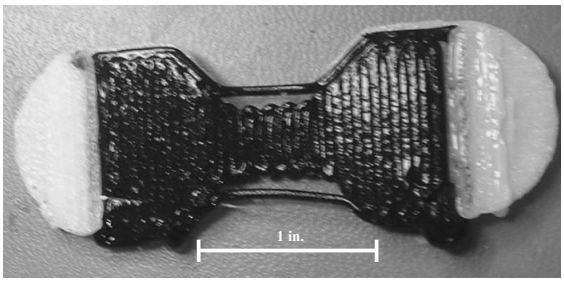


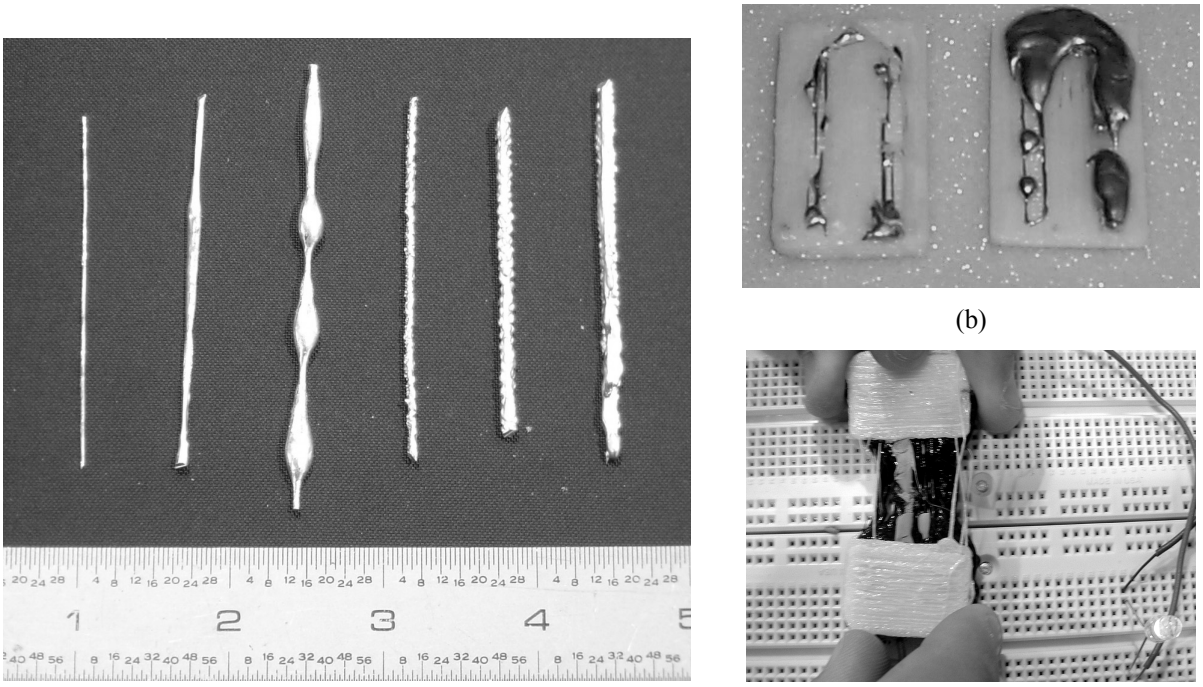
Figure 9: ABS and silicone elastomer flexure joint

Other Material/Functionality Experiments

As a demonstration of a multi-material functional mechanical assembly, a flexure joint was fabricated using ABS as the rigid end members and a 1-part, room-temperature vulcanizing (RTV) silicone as the flexible connection (Figure 9). The silicone is filled with carbon black to make it freestanding upon extrusion. The combination of electrical and mechanical functionality within the same freeform fabricated part is highly desirable and a number of approaches have been investigated [Ting *et. al.* 2001; Safari *et. al.* 2000]. Some initial qualitative experiments with applications of MC / metal powder pastes as functional materials outside of batteries have revealed that dehydration of the MC gel can lead to shrinkage and cracking of a deposited road of MC paste, and that adhesion to substrates also suffers after dehydration. A rudimentary electromechanical assembly was freeform fabricated as lines of silver / MC paste embedded in an ABS and silicone flexure joint (Figure 10c). This device successfully carried sufficient current to light an LED (~10mA), but was too delicate to survive much mechanical use due to cracking and detachment of the conductive paste.

Solder alloys are being investigated as a means of depositing wiring into components, and fabricating metal parts [Priest *et. al.*, 1997], and at least one commercial process exists which is capable of depositing solder alloy wiring onto a wide variety of substrates [Hayes *et. al.*, 1998]. Our previous experiments revealed that a large reservoir of molten eutectic alloy, for instance in a syringe, has the tendency to drain uncontrollably from the reservoir or to freeze in a nozzle. As an alternative approach, a solid-core, Pb-Sn solder wire was used as the feedstock for the wire-fed extrusion tool, and solder deposits were made directly on a build surface. Figure 10a depicts the results of these tests. It was found that there are small, separate regions of the parameter space in which it is possible to form either lines of overlapping frozen droplets of approximately 1mm in diameter (Figure 10a, right), or a very thin but continuous wire of approximately 250µm in diameter (Figure 10a, left). As a test of compatibility between

materials, several ABS and solder test coupons were freeform fabricated (Figure 10b). The deposited solder is electrically continuous for the entire "U" shape in the right-hand sample, which was produced at a fast feed rate, but only continuous about 2/3 of the total length of the "U" for the left-hand sample, which was produced at a much slower solder feed rate. The lead-tin solder does not wet ABS well, so making a robust interface between the two materials requires some surface preparation, or simply tightly embedding the solder within a channel in the ABS material. There is some indication that wetting may be improved by the use of indium-bearing alloys, although this has yet to be tested.



(a) (b) (c)

Figure 10: (a) Effect of deposition parameters on quality of solder alloy wiring, (b) partial success at embedding solder alloy wiring in thermoplastic part, and (c) flexure joint with silver/methylcellulose paste conductor

Conclusions

An uncased zinc-air cell has been successfully manufactured via freeform deposition techniques. The printed cell delivered at least 30mW for 2sec, from only 1gm of zinc slurry. A cell encased in ABS thermoplastic has also been successfully fabricated. The encased cell was able to deliver 5mW for more than 4 hours into a 100 Ohm load. Mechanical flexure joints have been freeform fabricated, as have a thermoplastic part with embedded metal wiring and a flexure joint with embedded silver/methylcellulose paste wiring which is capable of carrying more than 10mA of current. Obvious routes exist to improving the functionality and durability of all of these. The battery, flexure joints, and embedded wiring together demonstrate the feasibility of combining multiple materials into fully functional assemblies within a single freeform fabrication platform. Through further testing and optimization, higher performance cells are achievable, as are more sophisticated functional assemblies, leading the way to the production of immediately useable, freeform fabricated, electromechanical devices.

Acknowledgments

This work was supported in parts by the U.S. Department of Energy, grant DE-FG02-01ER45902. Thanks to Douglas Charles of Inco Technical Services for information on mixing ratios of methylcellulose and metal particles, and to Cordelia Rasa for information about methylcellulose products. D.C. thanks the NASA/NY space grant program for its support.

References

Danko, T. (1995), "Properties cellulose separators for alkaline secondary batteries", *Proceedings of the Tenth Annual IEEE Battery Conference on Applications and Advances(IEEE)*, Long Beach, CA, pp. 261-4

Duracell Incorporated (2001), "Duracell Zinc Air Batteries, Material Safety Data Sheet"

Fuller, S., Willhelm, E., Jacobson, J. (2002), "Ink-Jet Printed Nanoparticle Microelectromechanical Systems", *Journal of Microelectromechanical Systems*, Vol. 11 No. 1, February, pp.54-60

Harris, F., and Sieminski, D. (1999), "Recent Advances Enable Primary Zinc-Air for Portable Devices" *Wireless Symposium Spring 1999 Conference*, San Jose, CA, February, pp.22-26

Hayes, D.J., Cox, W.R., Grove, M.E. (1998), "Micro-jet printing of polymers and solder for electronics manufacturing," *Journal of Electronics Manufacturing.*, Vol. 8 Nos. 3-4, pp.209-16

Isaacson, T. (2003), "Printable Energy Source", Cornell University Master of Engineering Design Project Report

Linden, D. and Reddy, T., eds., (2002), Handbook of Batteries, 3rd Edition, McGraw-Hill

Lipson, H., Pollack J. B. (2000), "Automatic Design and Manufacture of Artificial Lifeforms", *Nature* 406, pp. 974-978.

Marcus H. L., Crocker, J.E., Harrison, S., Sun, L., and Shaw, L.L. (1998), "Gas (SALD) and Gas/Powder (SALDVI) Solid Freeform Fabrication (SFF)", Journal of Metals

Naimer, N., and Koretz, B., and Putt, R. (2002), "Zinc-Air Batteries for UAVs and MAVs", Electric Fuel Corporation, Auburn, AL. Available http://www.electric-fuel.com/defense/UVS02.pdf

Priest, J., Smith, C., and DuBois, P. (1997), "Liquid Metal Jetting for Printing Metal Parts", in Bourell, D. L., Beaman, J. J., Marcus, H. L., Crawford, R. H., and Barlow, J. W., (Ed.), *Proceedings of the Solid Freeform Fabrication Symposium*, Austin, TX

Safari, A., Danforth, S.C., Jafari, M., Allahverdi, M., Jadidian, B., Mohammadi, F. (2000), "Processing and properties of piezoelectric actuators developed by fused deposition technique", *ISAF 2000: Proceedings of the 2000 12th IEEE International Symposium on Applications of Ferroelectrics*, Vol. 1, pp.79-82

Swanson, W. J., and Hopkins, P. E. (1999), "Thin-wall tube liquifier", U.S. Patent 6,004,124

Tinker, L. (2002), "Air Electrode Performance in zinc-Air Batteries for Portable Products," *Proceedings of the Seventeenth Annual Battery Conference on Applications and Advances (IEEE)*, Long Beach, CA, p.221

Ting, F.P.Y., Gibson, I., and Cheung, W.L. (2001), "Study on selective laser sintering components with electrically conductive channels", in Bourell, D. L., Beaman, J. J., Marcus, H. L., Crawford, R. H., and Barlow, J. W., (Ed.), *Proceedings of the Solid Freeform Fabrication Symposium,* Austin, TX

Weiss, L. and Prinz, F. (1998), "Novel Applications and Implementations of Shape Deposition Manufacturing," *Naval Research Reviews*, Vol. 1, Office of Naval Research